2014-06-20

Aeration Effects on Impact: Drop Test of a Flat Plate

Mai, T

Proceedings of the International Offshore and Polar Engineering Conference
International Society of Offshore and Polar Engineers

Proceedings of the Twenty-fourth (2014) International Ocean and Polar Engineering Conference **www.isope.org**
Busan, Korea, June 15-20, 2014

ISBN 978-1 880653 91-3 (Set); ISSN 1098-6189 (Set)

Aeration Effects on Impact: Drop Test of a Flat Plate

Tri Mai, Deborah Greaves, Alison Raby
School of Marine Science and Engineering, Plymouth University
Plymouth, Devon, United Kingdom

ABSTRACT

Aeration effects on impact have been investigated by dropping a flat plate onto the water surface, in which the water is aerated to various degrees. An experimental study has been carried out in the newly commissioned Ocean Basin at Plymouth University's COAST Lab. The falling block comprises a rigid impact plate connected to two driver plates and its total mass can be varied between 32 kg and 52 kg. The impact plate is 0.25m long, 0.25 m wide and 0.012 m high. The impact velocity is varied between 4 m/s and 7 m/s. Preliminary results of the impact tests are presented here. Visualised results show that there are significant differences between jet formation after impact of the plate in pure water and in aerated water. There is significant reduction of the maximum pressures from those measured in pure water to those measured in aerated water.

KEY WORDS: Slamming; pressure; force; jet formation; aeration; void fraction.

INTRODUCTION

Slamming of an impact plate into pure water has been investigated over several decades using both theoretical and physical models. The first theory was developed by von Karman (1929) for a wedge and then for a horizontal plate impact into pure water. Later, Wagner (1932) developed the theory for a wedge with very small dead-rise angle, small enough not to trap air. There are a number of experimental studies undertaken to investigate slamming by dropping a wedge (Chuang, 1966a; Zhu, 1995; Zhao *et al.*, 1997), a horizontal bottomed body (Chuang, 1966a&b; Verhagen, 1967; Zhu, 1995; Bullock *et al.*, 2001; Kwon *et al.*, 2003; Oh *et al.*, 2009) and a horizontal circular cylinder (Lange *et al.*, 2011; Van Nuffel *et al.*, 2014) onto a still pure water surface. Smith *et al.* (1998) conducted a series of drop tests of a horizontal plate onto waves of different steepness.

If the compressibility of the water can be taken into account then the peak pressure at the instant of the impact of a horizontal plate onto still water, is equal to the acoustic pressure (von Karman, 1929) $p_a = \rho c v$, where ρ is the fluid density, c is the speed of sound in the fluid and v is the plate velocity just before the impact.

In practice, the maximum acoustic pressure never occurs because an air layer is trapped between the flat plate and the water surface and this air layer acts as a cushion layer. In the experiment of Chuang (1966a&b) the maximum impact pressure is found to be proportional to $\rho c_a v$, where c_a is the speed of sound in air. In the theory developed by Chuang (1966a & b), the compressibility of both the air and water was considered in a general solution of the problem. Since the maximum impact velocity was limited to 1.92 m/s, the finding in Chuang's tests may not necessarily apply to high impact velocity. The compressibility of the water and the elasticity of the body are neglected by Verhagen (1967). In his explanation, compressibility effects are neglected because the events of interest are expected to happen in a timescale of the order required by an acoustic wave in air to travel over a distance l, i.e., $\Delta t = l/c_a$, which is large compared with l/c (l is the half width of the flat plate). His experiments indicated that this assumption is fully justified. However, his experiments are limited to small values of the mass of the body compared with the added mass.

In particular, uncertainty exists in the understanding of the influence of the presence of air in the water (both entrapped pockets and entrained bubbles) leading to variability of wave impact pressures and forces. There are limited studies on the slamming impact onto aerated water so far (Bullock *et al.*, 2001; Lange *et al.*, 2011). In this paper, those aeration effects on impact have been experimentally investigated by dropping a flat plate onto the water surface, in which the water is aerated to various degrees.

EXPERIMENT

The experimental work has been carried out in the newly commissioned Ocean Basin at Plymouth University's COAST Lab (http://plymouth.ac.uk/pages/view.asp?page=39210). The ocean basin is 35 m long by 15.5 m wide and has a raisable floor that allows operation at different water depths up to 3 m. The falling block includes a rigid impact plate connected to two driver plates and its total mass can be varied between 32 kg to 52 kg. The impact plate is 0.25 m long,

0.25 m wide and 0.012 m high (Fig. 1 & Fig. 2) and the impact velocity is varied between 4 m/s and 7 m/s in the experiments in order to investigate the relationship between impact velocity, maximum pressure and force at impact. Force and pressures under the impact plate were measured during impact by an S-type load cell (Model 620) and five miniature pressure transducers (Model XPM10) installed on the impact plate. The velocity of impact was integrated from the measured data recorded by an accelerometer (Model 4610) mounted on the top of the impact plate. In addition, the impact velocity was also estimated from the drop height of the impact plate by formula $v = (2gh)^{0.5}$ and the effect of friction between the guide frame and the falling block wheels was observed. The configuration of the instrumentation on the impact plate is presented in Fig. 2.

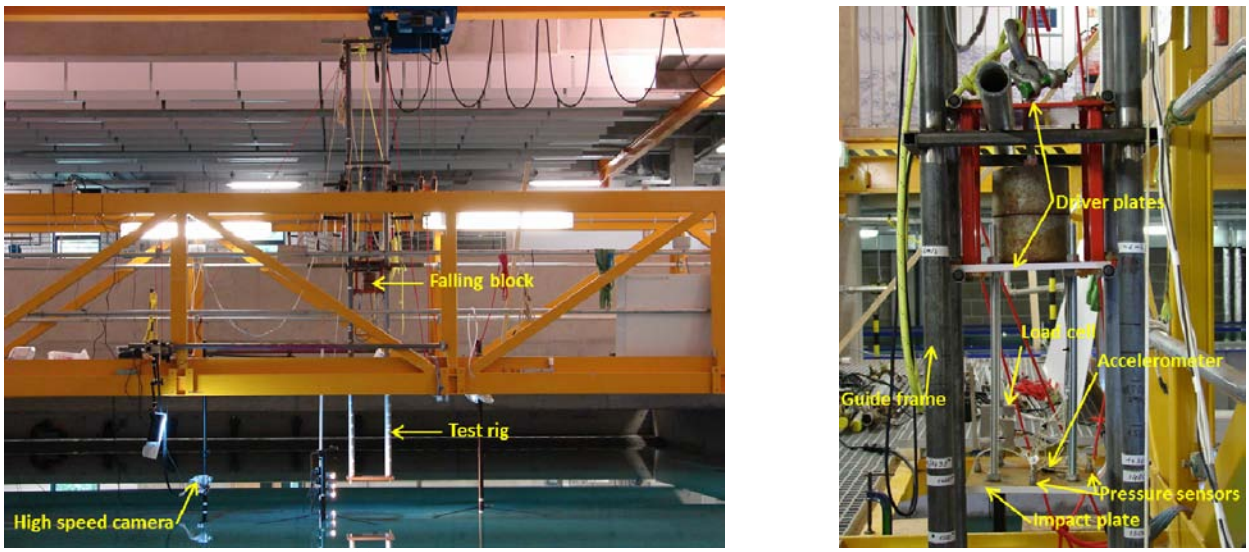

(a) (b)

Fig. 1: The test rig in the Ocean Basin (a) and the falling block and the instruments on the impact plate (b).

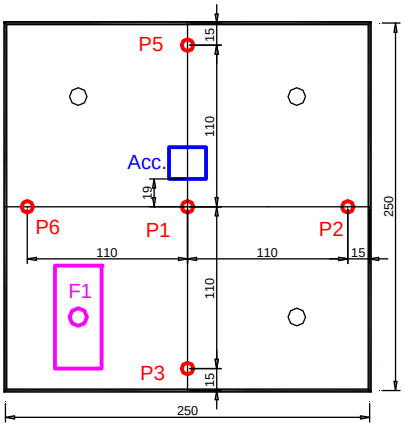

Fig. 2: Configuration of the instrumentation on the impact plate.

In addition, high speed photography (frame rate of 500 fps) was used to visualise the jets produced at impact and two underwater cameras were used to record the impact from underneath the plate.

Bubble Generation

Aerated water was achieved using a bubble generation system to introduce bubbles into the water column and thus obtain aerated water of different void fraction depending on the air injection pressure. The bubble generator was made of a perforated square clear plastic top-plate (dimensions of 0.54 x 0.54 x 0.002 m). The bottom plate and the sides of the bubble generator were also made of the clear plastic (see Fig. 3). The hole size on the top plate was drilled by laser cutter and has a diameter of around 0.2 mm. The hole spacing is 1 cm and distributed over an area of 0.495 x 0.495 m. To generate aerated water, the air from an air compressor (Fig. 4) was injected into the bubble generator via four air inlets. Snapshots of the aerated water generated by different air injection pressure levels are shown in Fig. 5 which shows that the increasing air injection pressure increases the bubble density.

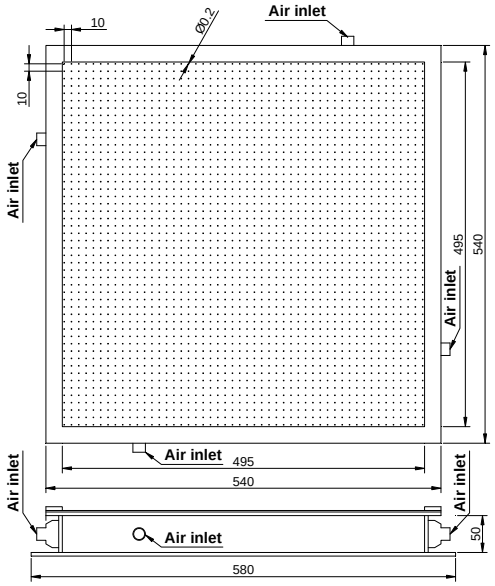

Fig. 3: The bubble generator (Units in mm).

Fig. 4: Air compressor.

Fig. 5: Aerated water generated at different air injections.

Void Fraction Estimations

Different methodologies for determination of the void fraction of aerated water are possible, including measurement of the speed of sound, volumetric method, hydrostatic pressure in aerated water, and by high speed photography to estimate bubble size, distribution and velocity. Each of these methods has their own disadvantages and difficulties, and in this paper the results obtained from the photography method and the volumetric method, are presented. The volumetric method (air flow rate measurement) is subjective in estimations and can be difficult to measure at the center of the bubble generator. Using the photography method, in which a high speed camera (Photron SA4) was used to record the development of bubbles, it can be difficult to see bubbles in a large depth of field. Therefore, a plastic plate was used to control the depth of field in the photography method.

In the volumetric method, the void fraction can be estimated by the following formula

$$\beta = \left(1 + \frac{1}{2\kappa}\frac{\Delta p}{p}\right)\frac{t_b}{t_{full}} \qquad (1)$$

where κ is the adiabatic coefficient,
Δp is the change in pressure given by the weight of the water column,
p is the surface pressure (atmospheric),
t_b is the time a bubble needs to reach surface after leaving the bubble generator,
t_{full} is the time needed to completely fill the cylinder with air.

A clear plastic cylinder was used to measure the air flow rate through the water body (Fig. 6a & b). The air flow rate of each aeration level was measured at nine spatial locations indicated in Fig. 6c.

In the photography method, the bubble development in water was recorded by a high speed camera Photron SA4, and the number of bubbles counted in a defined volume, based on a controlled depth of field of 0.05 m. The void fraction is equal to the total volume of all bubbles counted in the defined volume divided by the defined volume. It is observed that most bubbles have their shape of ellipsoid. The average bubble size varies from 2.3 mm to 6.6 mm.

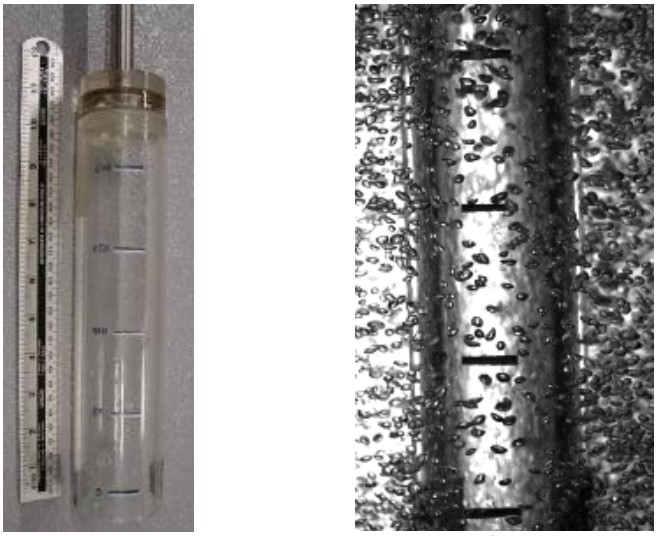

(a) (b) (c)

Fig. 6: The clear plastic cylinder and the measured locations.

The void fractions calibrated by the flow rate method and photography method are presented in Fig. 7. These void fractions have been calibrated in the wave flume and the ocean basin. The calibration has been applied for an air-water mixture depth of 25 cm from the water surface. As seen in Fig. 7, the void fractions calibrated in the wave flume and in the ocean basin are in reasonable agreement. In addition, the void fractions determined by the flow rate method and the photography method also agree well.

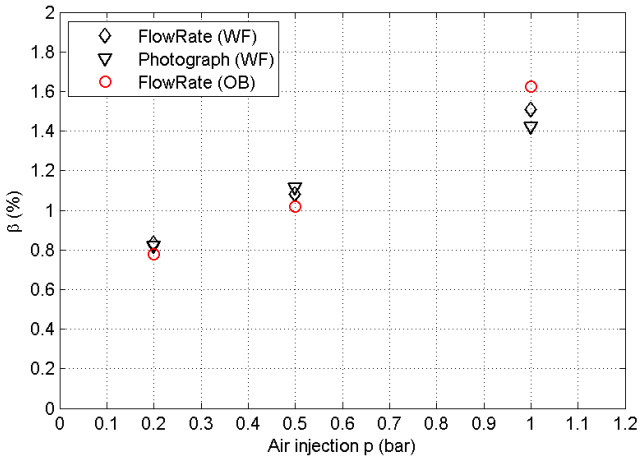

Fig. 7: Void fraction calibrated in the Wave Flume and Ocean Basin.

The standard deviation of void fraction measured using the flow rate method varies from 0.07% to 0.39% in the Ocean Basin and from 0.17% to 0.33% for calibration in the wave flume. By applying the photography method, the standard deviation of void fraction varies in the range of 0.06% to 0.1%.

RESULTS AND DISCUSSIONS

Drop Test in Pure Water

In Fig. 8, the jet formation due to the impact for the test case in pure water having impact velocity of 4.14 m/s and falling mass of 32 kg is shown at different time instants immediately before and after impact. Snapshots of the jets were taken using a high speed camera having frame rate of 500 fps. In this figure, six snapshots from t = 0.3 ms to 20.3 ms are presented. The snapshot at each time instant, t, was synchronised with the acceleration, velocity, pressures and forces measured and due to be presented in future work. The maximum velocity of the impact plate is obtained at t = 0 ms, therefore, the snapshot at t = 0.3 ms shows the position of the impact plate at just 0.3 ms before the instant at which the impact plate makes contact with the water surface. The second snapshot in Figure 8, taken at t = 4.3 ms shows the jet formation at 2.1 ms after the impact. The jet continues to grow as time progresses through the following snapshots in Figure 8, both in height and in diameter as the jet spreads out further from the plate. The height of the jet rises until at 20.3 ms it appears to hit the guide frame on the test rig. The maximum height of the jet in each of the snapshots is located at the centre of the plate side and reduces towards the corners of the plate. The root of the jet has a well-defined structure and shape and the tip of the jet exhibits break up into spray, which broadens with time.

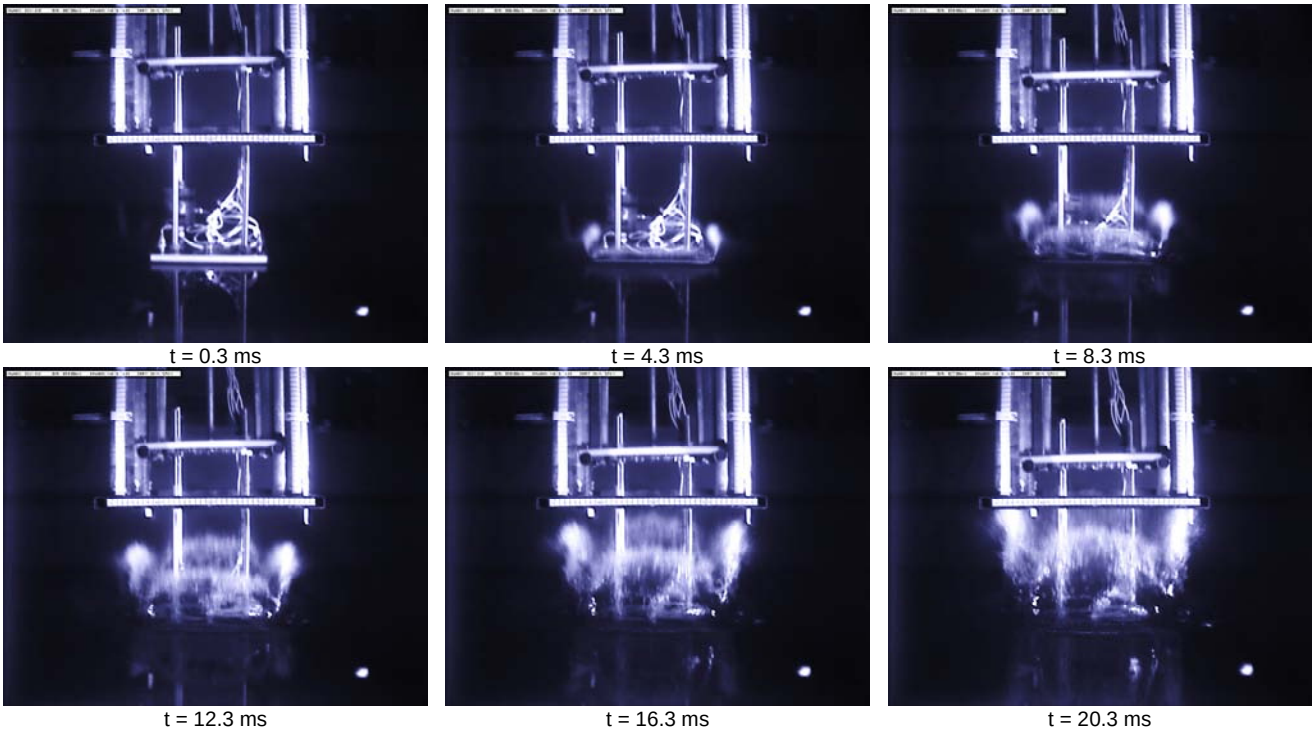

Fig. 8: Side view of the impact (β = 0 %, v = 4.14 m/s, m = 32 kg).

Fig. 9: Bottom view of the impact (β = 0 %, v = 4.14 m/s, m = 32 kg).

Fig. 9 shows the view from underneath the impact in pure water presented in Fig. 8. Snapshots in Fig. 9 were taken by a low frequency waterproof camera (frame rate of 30 fps). Although this camera was not synchronised with the high speed camera, which was used to visualise the jet formation near water surface in Fig. 8, we can observe features of the impact that are also evident in Fig. 8. The jet formation is clearly shown in these snapshots. The diameter of the jet can be seen to increase as the plate enters further into the water, corresponding to the spreading of the jet outwards from the plate shown in Fig. 8. Furthermore, in the final snapshot in Fig. 9, collapse of the jet can be observed. It should be noted that very different frame rates were used by the cameras generating snapshots in Fig. 8 & Fig. 9, and the final snapshot in Fig. 8corresponds to an instant shortly after the first snapshot in Fig. 9.

Symmetry of the jet formation during the impact onto pure water is quite clearly shown in the series of snapshots given in Fig. 8 & Fig. 9.

Drop Test in Aerated Water

The photographic results for the drop test onto aerated water recorded using a high speed camera are presented in Fig. 10 for the test where the impact velocity is 4.09 m/s and with a falling mass of 32 kg, from t = 1.24 ms to t = 21.4 ms with time step of 4 ms. Snapshot at each moment t was also synchronised with the acceleration, velocity, pressures and forces. The sequence shows that the jet formation under the impact in aerated water is very random and unstructured, unlike the case in pure water. This random nature of the jet formation is partly due to the instability of the aerated water surface, which is disturbed by the bubbles rising to the surface and never perfectly still.

In this case, the jet can be seen growing as the impact progresses. However, whereas in pure water, the jet grows in height through the sequence with a smooth well defined shape, in the case of aerated water impact, the jet extends further from the plate in the horizontal direction. Rather than being directed vertically, spray is thrown away from the

plate at low angles and does not reach the height of the guide frame.

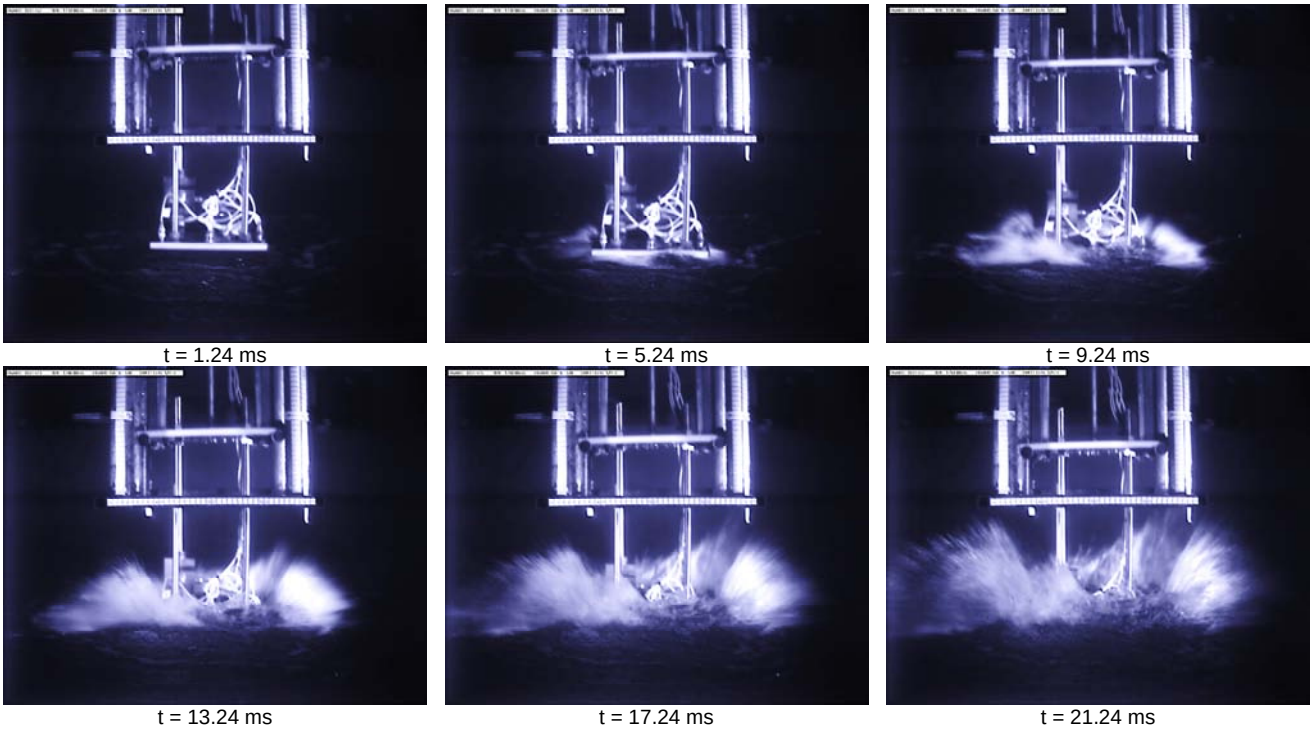

Fig. 10: Side view of the impact (β = 1.0 %, v = 4.09 m/s, m = 32 kg).

Fig. 11: Underwater oblique view of the impact (β = 1.0 %, v = 4.09 m/s, m = 32 kg).

In addition, the visualisation of the impact taken from under the water surface is presented in Fig. 11 for three different time instants after impact. These snapshots were taken by a low frequency waterproof camera and, as before, this camera could not be synchronised with the high speed camera and the data acquisition. The extent of the jet region can be seen to increase in width through the sequence of snapshots, although the jet has no clear structure.

Impact Pressures in Pure Water and Aerated Water

Time histories of impact pressures in pure water and aerated water are presented in Fig. 12. Fig. 12a presents pressures of a test, which has the impact velocity of 4.14 m/s and mass of 32 kg, in pure water. Fig. 12b presents pressures of a test in aerated water having 1% void fraction (the impact velocity of 4.09 m/s and mass of 32 kg). It is shown that the maximum impact pressure of P1, which is located at the center of the impact plate (see Fig. 2), decreases significantly from 14 bar obtained in pure water (Fig. 12a) to 1.5 bar obtained in aerated water (Fig. 12b). The other pressures have their maximum values reducing from about 6 bar of the test in pure water to about 2 bar of the test in aerated water. Pressures of P2, P3, P5 and P6 have their values obtained from the test in pure water are quite similar and this indicates that the impact plate has its deadrise angle of zero.

Analysis of the experimental data in detail is currently underway and results will be presented in future work.

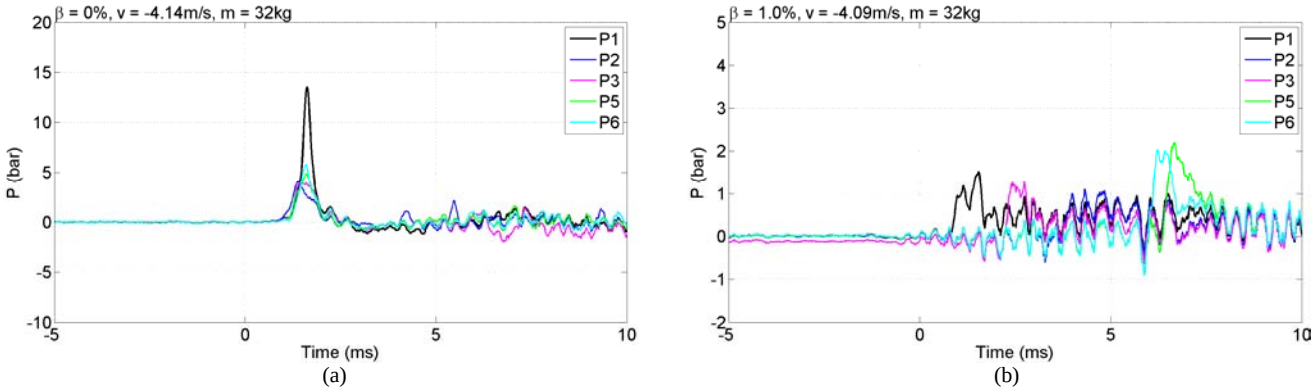

(a) (b)

Fig. 12: Time history of pressures of the impact in pure water (a) and in aerated water (b). Note: The vertical scales are different in the plots.

CONCLUSIONS

Slamming of a rigid flat plate onto pure water and aerated water has been investigated experimentally and preliminary results presented in this paper. The slamming event is reproduced experimentally by dropping a rigid plate, having mass of 32 kg and 52 kg, from various heights to obtain various impact velocities. The water was aerated by using a bubble generation system to obtain different aeration levels. The visualisation of jet formation under impact with still pure water and aerated water has been presented. The symmetry and well-defined structure of vertical jet formation due to the impact onto pure water is very clearly shown. In contrast, the jet formation due to the impact on aerated water is less well structured and spray is thrown out from the plate at low angles, causing a broader, broken jet. This is partly due to the unstable surface of the aerated water, which is disturbed by the bubbles and not perfectly horizontal as the plate makes contact with it. In addition, preliminary results show that there is significant reduction of the maximum pressures from those measured in pure water to those measured in aerated water. Analysis of the experimental data in more detail is currently underway and results will be presented in future work.

ACKNOWLEDGEMENTS

This study is a part of the FROTH (Fundamentals and Reliability of Offshore sTructure Hydrodynamics) project supported by the Engineering and Physical Science Research Council (EPSRC Grant EP/J012866/1). The collaborative partners include Oxford University, University of Bath, City University London and the Manchester Metropolitan University. The authors gratefully acknowledge the financial support provided by EPSRC and useful discussions with the partners.

REFERENCES

Bullock, G. N., A. R. Crawford, et al. (2001). "The influence of air and scale on wave impact pressures." *Coastal Engineering* 42(4): 291-312.

Chuang, S.-L. (1966a). "Slamming of rigid wedge-shaped bodies with various deadrise angles." David Taylor Model Basin, Washington DC, Report 2268.

Chuang, S.-L. (1966b). "Experiments on flat-bottom slamming", *Journal of Ship Research*, **10**(1), 10-17.

Kwon, S. H., Jung, D. J., Park, J. S., Pack, S. W., Chung, J. Y. (2003). "An Alternative Experiment for Slamming Using an Air Pressure Cylinder." *Proceeding of the 13th International Offshore and Polar Engineering Conference, ISOPE*, Honolulu, Hawaii, Vol 3, pp. 542-548.

Oh S. H., Kwon S. H., Chung J. Y. (2009), "A close look at air pocket evolution in flat impact." *Proc. of 24th International Workshop on Water Waves and floating Bodies*, Zelenogorsk, Russia.

Smith, N. J., Stansby, P. K. & Wright, J. R. (1998). "The slam force on a plate in free flight due to impact on a wave crest". *Journal of Fluids and Structures*, vol. 12, 183-196.

Van Nuffel, D., K. Vepa, et al. (2013). "A comparison between the experimental and theoretical impact pressures acting on a horizontal quasi-rigid cylinder during vertical water entry." *Ocean Engineering*.

Verhagen, J. H. G. (1967). "The impact of a flat plate on a water surface." *Journal of Ship Research* 10, 211–223.

von Karman, T. (1929). "The impact on seaplane floats during landing." National Advisory Committee for Aeronautics. *Technical Note*, vol. 321.

Wagner, H. (1932). "Über Stoß- und Gleitvorgänge an der Oberfläche von Flüssigkeiten." *ZAMM - Journal of Applied Mathematics and Mechanics / Zeitschrift für Angewandte Mathematik und Mechanik* 12(4): 193-215.

Zhu, L. (1995). "Structural Response of Ship Plates in Slamming-Drop Test Results and Analysis", University of Glasgow, Department of Naval Architecture and Ocean Engineering-*Reports*-NAOE.